Compact 60 GHz Hybrid Integrated Photoreceiver Module with 1.5-μm InAs Quantum Dot SOA

T. Umezawa, K. Akahane, N. Yamamoto, A. Kanno, and T. Kawanishi
National Institute of Information and Communication Technology (NICT)
4-2-1, Nukui-Kitamachi, Koganei, Tokyo 184-8795, Japan

Abstract— We have developed a 60-GHz hybrid integrated photoreceiver module using a quantum-dotbased optical semiconductor amplifier and a high-speed PIN photodetector for high-baud-rate opticalfiber communications. A high responsivity of 25 A/W and a high sensitivity of −20.5 dBm were achieved.

1. INTRODUCTION

With the data traffic carried over optical-fiber communication systems increasing every year, advanced modulation formats such as QPSK, 16QAM, and advanced parallel transmission technology such as space-division multiplexing are now implemented at baud rates of 25–30 Gbps [1]. Higher-baud-rate optical transmission is very attractive to improve the data rate capacity in long-reach to short-reach communications. Opto-electronic devices are a bottleneck for achieving high-frequency-response performance. For example, in photoreceivers using a transimpedance amplifier (TIA), the 3-dB bandwidth is limited by the TIA's bandwidth of 30 GHz [2]. Using an optical amplifier in place of an electric amplifier (TIA) makes high-baud-rate communication possible because of its wide frequency bandwidth. Very few compact photoreceiver modules operating at high baud rates have been reported. In this report, we present a compact photoreceiver module integrated with a PIN photodiode (PD) and 1.5-μm quantum dot (QD)Vbased semiconductor optical amplifier (SOA).

For QD emission devices such as QD lasers and QD SOAs, a low threshold current, temperature stability, high modulation bandwidth, low chirp, and a fast response is expected. This is because a QD is confined in all three dimensions [3]. We fabricated broad-area laser diodes comprising a 30-layer stacked InAs QD by using strain compensation. They had a high characteristic temperature (T_0) of 113 K at room temperature [4]. The devices exhibited ground-state lasing at 1529 nm. Because high-speed photo-emission carriers in the ground state are confined to a tiny quantum dot structure, a higher frequency response can be also be obtained. On the other hand, simulations using intermediate band models indicate a high conversion efficiency ($> 70\%$) in the QD solar cell [5]. In addition, we report results for the basic optical properties (large absorption coefficient, low dark current, and avalanche multiplication effect) of the high-density QD absorption layer [6]. A monolithic integrated photoreceiver with a high-density QD active layer in an SOA, and a PD is the ideal device to improve sensitivity at higher baud rates. We designed and investigated the basic properties of a hybrid integrated photoreceiver with a QD-SOA as the first stage.

2. FABRICATION

Highly dense InAs QDs were fabricated using the conventional solid-source molecular beam epitaxy (MBE) technique. The stacked QD structures were then fabricated on an N+InP(311)B substrate. By using the strain compensation technique [7], a 20-layer stack of high-density InAs QD, and 20-nm-thick InGaAlAs spacer layers were grown on a 150 nm n^+ InAlAs buffer layer, where the InAs QD density was greater than $1.3 \times 10^{12}\,\mathrm{cm}^{-2}$. A 2.7-μm ridge waveguide was fixed at an angle of 6° to the surface, normal to the cleaved facet, in order to reduce the reflection of light. The cavity length was designed as 2 mm. We obtained the following optical characteristics: an amplified spontaneous emission (ASE) wavelength in the range 1480–1580 nm, a full width half maximum (FWHM) of 40 nm in the ASE peak, and a high gain greater than 20 dB [8].

We report the possibility of using an InAs QD absorption layer for high-speed PDs, which exhibits a high absorption coefficient, low dark current, and avalanche multiplication effect. However, a large coupling loss between the QD-SOA and the waveguide QD-PD is expected because the photoreceiver module used in this experiment was designed using microlens coupling in free-space optics. To overcome this, a back-illuminated InGaAs-based PIN-PD with a large photodetective area (diameter: 10 μm) was designed. To obtain a larger 3-dB bandwidth and a high responsivity, an optimum InGaAs absorption layer thickness was employed in the PIN structure. The measured responsivity and the 3-dB bandwidth using wafer testing were as high as 0.4 A/W at 1550 nm and 60 GHz, respectively.

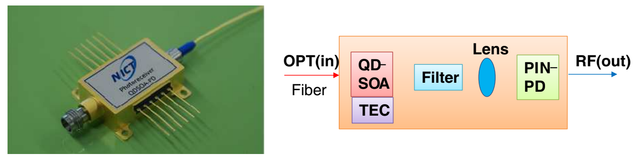

Figure 1: 60-GHz hybrid integrated photoreceiver with a QD-SOA (left part), and the schematic diagram for the module structure (right part).

A high-speed butterfly package for a hybrid integrated photoreceiver was carefully designed for achieving a low insertion loss of 0.5 dB and a low return loss of 10 dB at 65 GHz, using electromagnetic simulations. All optical components (PD, SOA, Thermo Electric Cooler, 4 lenses, filter and other parts) were implemented in a compact package (W : 18 mm × D : 29 mm × H : 9 mm). Then, each device was optically coupled using free-space optics. The emitted light from the QD-SOA was filtered by a 1530- nm optical band-pass filter and focused on a 5-µm spot with a PD. The operational temperature was controlled at 20–40°C (see Fig. 1).

3. RESULTS AND DISCUSSION

For the photoreceiver, the PD's DC responsivity at 1532 nm was measured with a QD-SOA driving current of 200 mA and an optical input power of −20 dBm. The output power from the QD-SOA was measured with a micro-optics apparatus. Although, a responsivity of 0.4 A/W was expected during wafer testing, a 20% variation (0.32–0.4 A/W) was seen in the photoreceiver. It was caused by an optical mismatch between the designed photodetective area (diameter: 10 µm) and the incident beam spot size (diameter: 5 µm). Fig. 2 shows the photoreceiver's responsivity dependence on the SOA driving currents in the range 0–400 mA. At 400 mA, a high responsivity of 14–25 A/W without saturation in the curve was observed. It was different from the expected responsivity of 40 A/W (PD responsivity: 0.4 A/W, SOA gain: 20 dB) because of the characteristics variation in the SOA wafer. The peak ASE wavelength in the implemented SOA die was 1500 nm, which exhibited a blue shift of 32 nm from the averaged ASE peak wavelength in the wafer. Comparing the optical gain at 1500 nm with that at 1532 nm, the gain at 1532 nm would be as small as 4.5 dB.

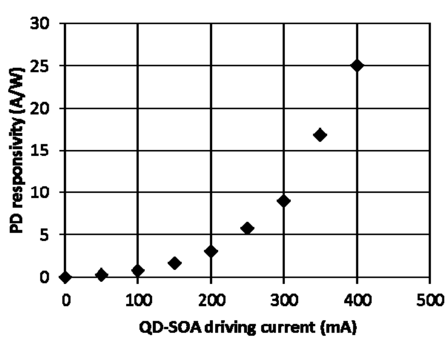

Figure 2: PD responsivity of the photoreceiver module vs. the QD-SOA driving current.

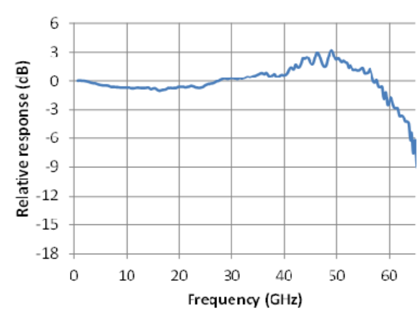

Figure 3: Frequency response for photoreceiver module for a QD-SOA driving current of 200 mA.

Next, the frequency response of the PD at a reverse bias voltage of −2 V was measured for the photoreceiver modules with a QD-SOA by a Lightwave Component Analyzer (LCA). By applying a driving current of 200 mA to the QD-SOA at a wavelength of 1532 nm, the 3-dB bandwidth ($f_{3\mathrm{dB}}$) of 62 GHz was obtained, as shown in Fig. 3. Note that a photoreceiver without a QD-SOA had the same 3-dB bandwidth under the same testing conditions. The measured $f_{3\mathrm{dB}}$ are in good agreement with the calculated $f_{3\mathrm{dB}}$ of 56 GHz, which was estimated from the CR time constant and the carrier drifting time in the depletion layer.

A bit error rate (BER) test was carried out to study the optical noise affection in QD-SOA. It is well known that the quality factor (Q) or the signal-to-noise ratio (SNR) is proportional to the BER as described in Equations (1) and (2). We investigated the BER at 10 Gbps (NRZ format, PRBS = $2^{31} - 1$). When a large ASE noise was generated in the QD-SOA, a curving BER characteristic with noise floor was expected. Fig. 4 shows the BER characteristics with driving currents of 200 mA, 300 mA, and 400 mA in the QD-SOA. For a BER = 1×10^{-12}, sensitivities of −13.5 dBm, −17 dBm, −20.5 dBm were observed, respectively. The sensitivity of −20.5 dBm at a driving current of 400 mA is useful for a commercially available 10-Gbps ROSA (−18 dBm). By tuning the wavelength range in the QD-SOA to the ASE peak, the sensitivity of 4.5 dB can be improved. (−25 dBm)

$$\mathrm{BER} = 1/2 * \mathrm{erfc}(Q/\sqrt{2}) \quad (1)$$

$$\mathrm{SNR} = 4Q^2 \quad (2)$$

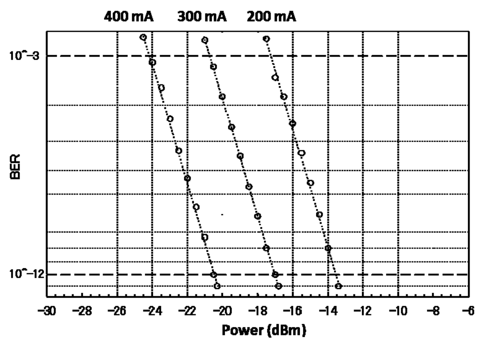

Figure 4: BER curve at 10 Gbps (NRZ) at various QD-SOA driving currents.

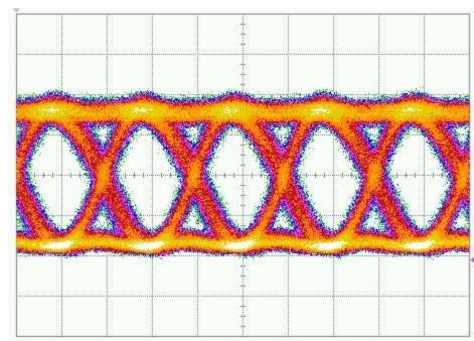

Figure 5: Eye diagram at 50 Gbps, optical input power of −7 dBm, SOA driving current of 290 mA. (Time: 10 psec/div).

The photoreceiver, which consists of a 60-GHz PIN-PD and a wide frequency bandwidth QD-SOA, can be expected to work well under high-baud-rate conditions (> 60 Gbps). To test the high-baud-rate performance, an eye diagram test at a maximum baud rate of 50 Gbps (NRZ) was conducted with optical input power ranging from −20 dBm to +0 dBm. In Fig.5, the eye diagram at an input power of −7 dBm is shown. High quality eye diagrams with clear eye opening were found in range from 10 Gbps to 50 Gbps. In results, we strongly suppose that the BER performance with high sensitivity could be obtained up to 50 Gbps. The results suggest that the hybrid photoreceiver is a good candidate for higher-baud-rate opticalfiber communications. Furthermore, it would not be difficult to make a monolithic integration of the QD using the SOA and PD.

4. CONCLUSION

We have a developed 60-GHz hybrid integrated photoreceiver, which consists of a 1.5-μm QD-SOA and a high-speed PIN-PD. A maximum responsivity of 25 A/W at a QD-SOA driving current of 400 mA and a 3-dB bandwidth of 62 GHz was achieved. A high sensitivity of −20.5 dBm was obtained through a BER test at 10 Gbps, and a clear eye diagram at 50 Gbps was also obtained. We believe that this design is well suited for high-baud-rate optical-fiber communications. A monolithic integrated device combining the QD-SOA and QD-PD will show higher responsivity. Further, the photoreciever can be used for radio over fiber communications.

ACKNOWLEDGMENT

This study was conducted as a part of a research project supported by the Japanese Government funding for "R&D to Expand Radio Frequency Resources" by the Ministry of Internal Affairs and Communications.

REFERENCES

1. Igarashi, K., et al., *ECOC Tech. Dig.*, Mo.3.A2.
2. Data sheets of HMC6590, Hittite, http://www.hittite.com/products/view.html/view/HMC6590.
3. M.Ishida, et al., *CLEO Tech. Dig.*, CM1I.2, 2012.
4. K.Akahane, et al., *IEEE Photonics Tech. Lett.*, Vol. 22, No. 2, Jan. 15, 2010.
5. Y.Arakawa, et al, *Ext. Abstr. (58nd Spring Meet., 2011)*, Japan Society of Applied Physics and Related Societies, 24a-KW-10 (in Japanese).

6. T.Umezawa, et al., *Appl. Phys. Express*, Vol. 7, 032201, 2014.
7. K.Akahane, et al., *Phys. Status Solid A*, Vol. 208, No. 2, 425–428, 2011.
8. K.Akahane, et al., *Jap. J. Appl. Phys.*, Vol. 53, 04EG02, 2014.